Magnetic Exchange Interactions in Oxo-Bridged Diiron(III) Systems: Density Functional Calculations Coupling the Broken Symmetry Approach

Zhida Chen,*,† Zhitao Xu,‡ Lei Zhang,† Feng Yan,† and Zhenyang Lin‡

State Key Laboratory of Rare Earth Materials Chemistry and Applications, Department of Chemistry, Peking University, Beijing 100871, China and Department of Chemistry, Hong Kong University of Science and Technology, Clear Water Bay, Kowloon, Hong Kong

Received: March 7, 2001; In Final Form: July 23, 2001

The calculations on magnetic exchange interaction of $Cl_3FeOFeCl_3^{2-}$ and the related modeling compounds were performed by using the density functional theory coupling the broken symmetry approach. The calculated results show the absence of a direct Cl_3Fe---$FeCl_3$ magnetic coupling and the effect of the terminal Cl ligands on magnetic exchange interaction in $[Fe-O-Fe]^{4+}$, while the protonation of μ-oxo bridge reduces significantly the magnetic coupling constant J value. On the other hand, the J value is insensitive to variation of the Fe−O−Fe angle; however, the dependence of the J value on the Fe−O distance can be expressed as an exponential function, while the J value keeps a constant to the variation of the O−H distance in the μ-hydroxo and μ-aqua bridges. Molecular orbital interaction is applied to explain the magnetic exchange interaction in μ-oxo bridged iron(III) dimers. The validity of qualitative magneto−structural correlation for the models used is further confirmed by full geometry optimization.

Introduction

In the past decade, the magneto−structural correlation of binuclear compounds of transition-metal ions has received much attention both experimentally and theoretically.[1−3] Most of the transition-metal binuclear compounds are bridged with a wide variety of bridge ligands, such as chloro, azido, oxo, hydroxo, oxalato, or more complex bridges, in the manner of singly, doubly, or multiply bridging. Thus, the magnetic properties for the binuclear compounds are known to depend mainly on the particular metal ions, the chemical nature of the bridging ligands, and bridging geometries. One of the most extensively studied families experimentally is hydroxo-bridged copper(II) binuclear compounds. These copper(II) binuclear compounds are also of particular interest from a theoretical point of view because of their simplest magnetic interaction involved in only two unpaired electrons.[4] Magneto−structural correlation for chromium(III) dimers with the double hydroxo bridges has also been established.[5] Recently, several reports have been devoted to oxo-bridged iron(III) dimers.[6] Some attempts to correlate the experimentally determined magnetic coupling constant J to the bridging geometry for oxo-bridged iron(III) dimers have been reported.[7] The magnetic interaction of these compounds experimentally are found to be anti-ferromagnetic, where there are 5 unpaired electrons for each iron(III) ion with a high spin state, differing from only one unpaired electron involved in each copper(II) ion for the hydroxo-bridged copper (II) dimers. Thus, in the case of iron (III) dimers, magnetic behavior is less easy to rationalize, even some conflicting conclusions occur. A rapid decrease of magnetic coupling constant J with a decrease of Fe−O−Fe angle ϕ from 180° was expected by Gerloch,[7g] while Holm observed a slow decrease of J with ϕ decreasing.[7e] No correlation of J with the bridging angle was also reported.[7f] In connection with the bridging ligand−metal distance dependence of J, a following correlation has been suggested [7d]

$$-J = Ae^{-BP} \tag{1}$$

with $A = 8.763 \times 10^{11}$ cm^{-1}, $B = 12.663$ Å^{-1}, and P is half the shortest superexchange pathway between the two iron (III) ions. Recently, the magneto−structural relationship has been also found in ab initio calculations for $Cl_3FeOFeCl_3^{2-}$,[7c] which is a slight increase of J upon lowering the Fe−O−Fe angle and a qualitatively exponential dependence of J on the Fe−O distance.

Experimentally, the magnetic coupling constants $-J$ (in Hamiltonian $\hat{H} = -2J\hat{S}_1\cdot\hat{S}_2$) for the vast majority of oxo-bridged diiron (III) compounds fall into the 80−120 cm^{-1} range.[6a] However, in contrast to oxo-bridged diiron(III) compounds, the μ-hydroxo diiron(III) compounds have $-J$ values in the 7−17 cm^{-1} range, with the bis(μ-hydroxo) diiron(III) compounds being at the lower end of this range.[6a] Though additional one or two carboxylate bridge ligands may exist in the oxo-bridged diiron (III) compounds studied, they play a negligible role as the exchange pathways compared to the bridging oxo.[6a,7i]

The rather confusing situation mentioned above arouses us to take again into account the magneto−structural correlation for the oxo-bridged iron(III) dimers. It has recently been demonstrated that the broken symmetry approach, proposed by Noodleman,[8] can offer an approximation to a limited configuration interaction and can be successfully applied to study the magnetic properties of binuclear and tetranuclear compounds.[4b,4d−4f,8] In our calculations, the density functional theory (DFT) coupling the broken symmetry approach (BS) is adopted. In connection with calculations of magneto−structural correlation, the singly μ-oxo bridged anion $Cl_3FeOFeCl_3^{2-}$ in the staggered conformation is chosen as a pattern of the oxo-bridged iron(III) dimers.[6f] In a recent report, Rappe et al. calculated

* To whom correspondence should be addressed. Fax: +86-10-62751708. E-mail: zdchen@pku.edu.cn.
† Peking University.
‡ Hong Kong University of Science and Technology.

10.1021/jp010864m CCC: $20.00
Published on Web 09/26/2001

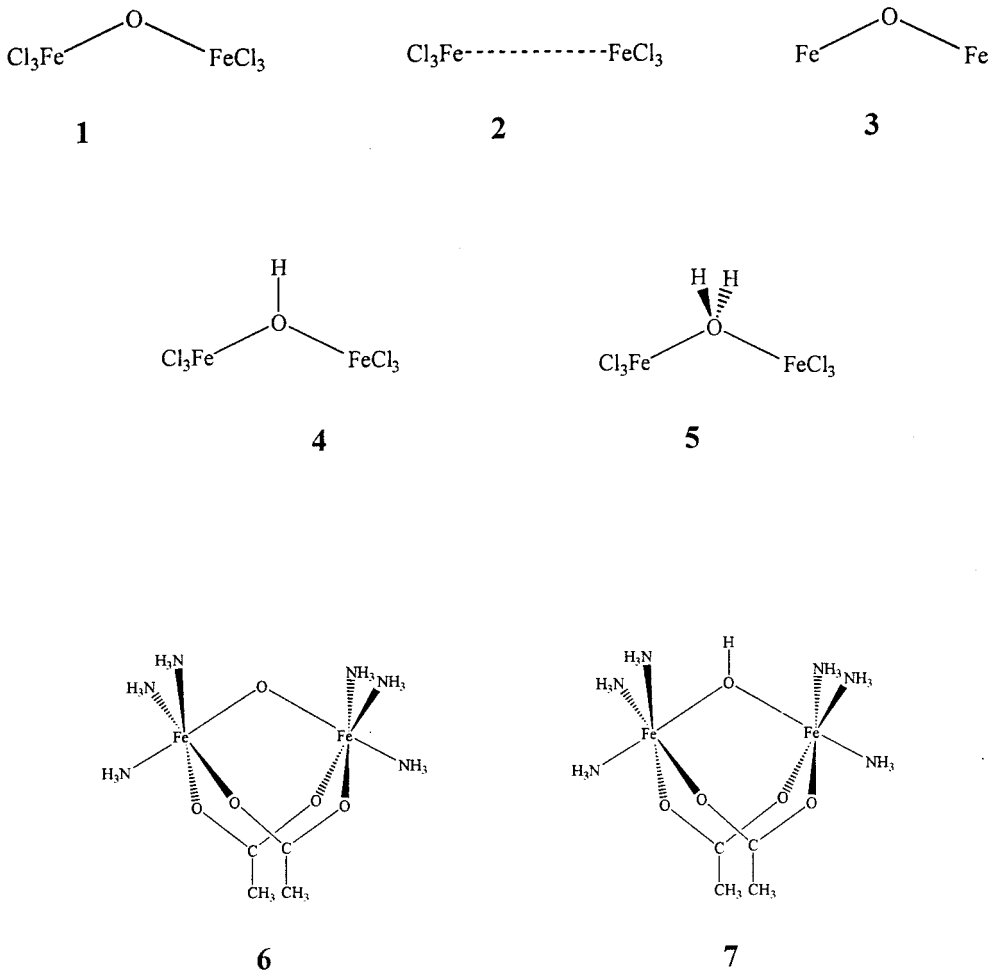

Figure 1. The scheme of the calculated models.

magnetic behavior for this anion with the eclipsed conformation by using ab initio method.[7c] However, in the case of the eclipsed conformation, a stronger, nonbonding repulsive interaction exists between the terminal chlorine atoms coordinated to each iron(III) center so that the magnetic behavior is complicated as Fe−O distance or Fe−O−Fe angle decrease.[7c] The staggered conformation is also a known important conformation for $Cl_3FeOFeCl_3^{2-}$ experimentally.[6a,6f] Recently, we obtained another new μ-oxo bridged iron(III) dimer with the $Cl_3FeOFeCl_3^{2-}$ anion in the staggered conformation.[9] In the present paper, the magneto−structural correlation is revisited and further extended to the influence of protonation of oxo-bridge ligand as well as to the case of multiply bridged iron(III) dimer; meanwhile, the molecule orbital theory is applied to explain the magnetic behavior observed experimentally.

Computational Details

Description of the Models. In our calculations, the models **1**−**7** studied are shown in Figure 1, in which the models **1**−**3** are built to analyze the dependence of the exchange coupling constants J on the μ-oxo bridging ligand and terminal Cl ligands. Model **1** is the anion of the $[Fe^{II}(bipy)_3][Fe_2OCl_6]$.[6f] Because the magnetic behavior is sensitive to any tiny deviation of the molecular structure studied, the geometry structure of model **1** in the staggered conformation is directly taken from X-ray crystallography analysis[6f] without optimization for structural parameters. The Fe−O distance is 1.765 Å, and the Fe−O−Fe angle is 148.1°. As shown in previous reports,[4f,5a] the inclusion of the counterions in the calculations of the exchange coupling constant appears to be important only when these counterions are coordinated to the metallic centers.[4f,5a] In the case of $Cl_3FeOFeCl_3^{2-}$, the effect of the counterions on the magnetic exchange interaction can be apparently neglected, except for the effect of the counterions on structural parameters of $Cl_3FeOFeCl_3^{2-}$. In the analysis of magneto−structural correlation, it is useful to employ model structures because the main aim in this case is to study the variations of the magnetic behavior with structural parameters, rather than to calculate the coupling constant. In the cases of models **2** and **3,** the μ-oxo bridging ligand and terminal Cl ligands are respectively omitted while keeping the other pieces of the molecule fixed to inspect dependence of exchange coupling constant on these ligands. Model **4** is protonation of the bridge O ligand, leading to form a hydroxo OH bridge ligand, where only the O−H distance is optimized. Attaching another proton again to the OH bridge ligand leads to model **5**, in which the O−H distances and the H−O−H angle are also optimized. Model compounds **6** and **7** with simplified terminal ligands are designed to model the real molecules $[(HB(pz)_3)FeO(OAc)_2Fe(HB(pz)_3)]$[6g] and $[(HB(pz)_3)Fe(OH)(OAc)_2Fe(HB(pz)_3)]^+$.[6e] The structural parameters of the two Fe centers and bridge ligands for models **6** and **7** are directly adopted from the experimental data of $[(HB(pz)_3)FeO(OAc)_2Fe(HB(pz)_3)]$[6g] and $[(HB(pz)_3)Fe(OH)(OAc)_2Fe(HB(pz)_3)]^+$[6e], respectively, to examine further the effect of protonation of the bridge O ligand in μ-oxo bridged iron(III) dimer with two additional supporting μ-carboxylate bridges. In the case of $[(HB(pz)_3)FeO(OAc)_2Fe(HB(pz)_3)]$, the Fe−O distance is 1.785 Å and the Fe−O−Fe angle is 123.6°. For $[(HB(pz)_3)Fe(OH)$-

$(OAc)_2Fe(HB(pz)_3)]^+$, the Fe−O distance is 1.956 Å and the Fe−O−Fe angle is 123.1°.

Calculation on Exchange Coupling Constant. The magnetic interaction between iron ions is studied on the basis of density functional theory coupling with the broken symmetry approach (DFT-BS). The exchange coupling constants *J* have been evaluated by calculating the energy difference between the high-spin state (E_{HS}) and the broken-symmetry state (E_{BS}) (assuming the spin Hamiltonian is defined as $\hat{H} = -2J\hat{S}_1\cdot\hat{S}_2$), according to the following expression:[8a]

$$E_{HS} - E_{BS} = [-S_{max}(S_{max}+1) + \sum_{S}^{S_{max}} A_1(S)\cdot S(S+1)]J \quad (2)$$

where *S* corresponds to the spin states of the molecule studied and $A_1(S)$ stands for squares of Clebsch−Gordan coefficients. In the cases of the anion $Cl_3FeOFeCl_3^{2-}$, where S_1=5/2 and S_2=5/2, from the spin project method we get the expression as follows:

$$E_{HS} - E_{BS} = -25J \quad (3)$$

where positive value of the coupling constant *J* indicates a high-spin ground state with parallel spins (i.e., ferromagnetic character). For negative value of *J*, the broken-symmetry state is lower in energy with opposite spins on iron ions giving rise to anti-ferromagnetic behavior.

All the calculations have been performed using the Amsterdam Density Functional (ADF) package version 2.3.[10] The local density approximation (LDA) with local exchange and correlation potentials makes use of Vosko, Wilk, and Nusair (VWN) correlation functionals.[11] Becke's nonlocal exchange correction[12] and Perdew's nonlocal correlation correction[13] are added in each SCF consistent cycle. We have used the IV basis sets in ADF, containing triple-ζ basis sets for all atoms and a polarization function from H to Ar atoms. The frozen-core (FC) approximation for the inner-core electrons is used. The orbitals up to 2p for Fe and Cl atoms and up to 1s for O, N, and C atoms are kept frozen. The numerical integration procedure applied for the calculations is the polyhedron method developed by Velde and co-workers.[14]

Results and Discussion

A. Effect of Bridging and Terminal Ligands. Using DFT-BS, the exchange coupling constant between the two iron(III) centers in $Cl_3FeOFeCl_3^{2-}$, model **1**, is calculated to be −244 cm^{-1}. The sign of the *J* value is minus, suggesting an anti-ferromagnetic character between two iron(III) centers. The qualitative agreement between the calculated and experimental values (−134 cm^{-1})[6a] for the coupling constant *J* is good though there is a difference in absolute value. The particular emphasis in our calculations is placed on analysis of the dependence of exchange coupling constants on the specific changes in structures.

To examine the effect of the bridging ligand, we omitted the bridge O atom and fixed the other pieces of the molecule (model **2**). The relatively small *J* value (−25.6 cm^{-1}) is obtained for the no-bridged Cl_3Fe---$FeCl_3$ species, model **2**.This *J* value could be considered as the absence of direct exchange interaction between the two $[Cl_3Fe]$ fragments. In comparison with the calculated *J* value (−244 cm^{-1}) of model **1**, the small *J* value also indicates that the bridging O atom plays a crucial role in determining the magnetic exchange interaction between the two iron(III) centers.

When all the terminal Cl ligands are removed and the same calculations are done for the naked $[Fe-O-Fe]^{+4}$ fragment (model **3**), the exchange coupling constant *J* remains almost unchanged (−247.2 cm^{-1}), suggesting that the terminal ligands do not have significant effect on the Fe---Fe exchange coupling.

B. Protonation of μ-Oxo Bridge. The protonation of the μ-oxo bridge, leading to a hydroxo OH bridging ligand (model **4**), provides an example to compare the effect of different bridges on the exchange coupling interactions. In our calculations, it is shown that directly attaching a proton to the bridge O atom results in remarkable weakening of the anti-ferromagnetic exchange interaction between the two iron(III) centers, with a calculated *J* value of −110cm^{-1}, less than −244 cm^{-1} of $Cl_3FeOFeCl_3^{2-}$ in absolute value. The *J* value remains constant (−110cm^{-1}) when the bridge H−O distance changes from 0.95 Å to 1.3 Å. Attaching another H^+ again to the OH bridge ligand, leading to form a bridge H_2O ligand (model **5**), further weakens the anti-ferromagnetic exchange interaction between the two iron(III) centers ($J = -62$ cm^{-1}), while the exchange coupling interaction between the two iron(III) centers is also insensitive to the H−O distance in the bridge H_2O ligand. When the H−O distance changes from 0.95 Å to 1.00 Å in model **5**, the *J* value remains constant (−62 cm^{-1}). It appears that the DFT-BS calculations on the protonation of the μ-oxo bridged iron(III) dimer reproduce the experimental observation of magnetic behavior for the μ-oxo and μ-hydroxo bridged iron-(III) dimers.[6a]

C. $(NH_3)_3FeO(OAc)_2Fe(NH_3)_3$ (6) and $(NH_3)_3Fe(OH)(OAc)_2Fe(NH_3)_3$ (7). It has been found experimentally that the anti-ferromagnetic coupling constant of the $[(HB(pz)_3)FeO(OAc)_2Fe(HB(pz)_3)]$ (−121 cm^{-1})[6a,6e] is more negative than that of $[(HB(pz)_3)Fe(OH)(OAc)_2Fe(HB(pz)_3)]^+$ (17 cm^{-1}).[6e] In the previous reports,[6a,6c] this increase of the anti-ferromagnetic exchange interaction in $[(HB(pz)_3)FeO(OAc)_2Fe(HB(pz)_3)]$ compared to $[(HB(pz)_3)Fe(OH)(OAc)_2Fe(HB(pz)_3)]^+$ has been attributed to the shorter Fe−O distance (1.784 Å) when compared with 1.956 Å in $[(HB(pz)_3)Fe(OH)(OAc)_2Fe(HB(pz)_3)]^+$. Nevertheless, both Fe−O distances and protonation of the bridge O ligand may have significant influence on the magnetic exchange interaction between the two iron(III) centers. To further understand the influence of the different bridge ligand in these iron(III) dimers, two model compounds of the iron(III) dimers, models **6** and **7**, have been designed and calculated with DFT-BS mentioned above.

For multiply bridged (μ-oxo) diiron compounds, the magnetic coupling constant *J* is related to the shortest superexchange pathway between the iron centers and the bridge ligand. Experimentally, the oxo bridge in model **6** is the dominant mediator of magnetic exchange coupling, while the hydroxo bridge in model **7**, as the shortest superexchange pathway of this compound, mediates a smaller degree of anti-ferromagnetic coupling than does an oxo bridge. As expected, the anti-ferromagnetic exchange interaction between the two iron(III) centers for model **6** is calculated to be stronger (−329 cm^{-1}) than that of model **7** (−75 cm^{-1}).

To examine the influence of the hydrogen atom in the μ-hydroxo ligand, we delete the H^+ in the μ-hydroxo ligand for model **7** (giving model **7′**) while keeping the other pieces of the molecule fixed. This deprotonation leads to a remarkable increase of the anti-ferromagnetic exchange interaction (from −75 to −198 cm^{-1}) between the two iron(III) centers. Consistently, attaching a proton (H^+) to the μ-oxo ligand for model **6**, similar to model **7**, and keeping the other pieces of the molecule fixed (giving model **6′**) leads to significant weakening of the

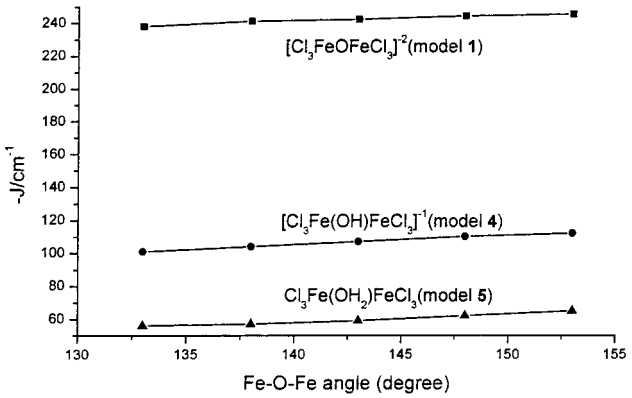

Figure 2. Dependence of the calculated magnetic coupling constants J in models **1**, **4**, and **5** on Fe−O−Fe angle.

anti-ferromagnetic coupling (from −329 to −189 cm^{-1}). Though the model pair **7** and **6′** as well as the model pair **7′** and **6,** respectively, have the same geometrical configuration of the model pair, there are different bridge distances in the model pair: the Fe−O distance of 1.956 Å for models **7** and **7′** and the Fe−O distance of 1.784 Å for models **6** and **6′**. Thus, the J values of model **7′** (−198 cm^{-1}) and model **6** (−329 cm^{-1}) differ from each other, and the J values of model **7** (−75 cm^{-1}) and model **6′** (−189 cm^{-1}) differ from each other. So far, it can be confirmed that the proton in the bridges indeed plays a very important role in the magnetic exchange interaction between the two iron(III) centers except the dependence on the Fe−O distance in the bridge for these compounds studied.

D. Magneto−Structural Correlation. Usually, short Fe−O(oxo) distances are characteristic of the diferric Fe−O−Fe unit. Fe−O distances range from 1.73 to 1.82 Å, in which the average for the 4-coordinate iron(III) dimers is somewhat shorter at 1.75 Å. The Fe−O−Fe angle in the μ-oxo iron(III) dimers is quite flexible, ranging from 114° to 180°. In the case of $Fe^{II}(bipy)_3[Fe_2OCl_6]$,[7f] the Fe−O distance is 1.765 Å and the Fe−O−Fe angle is 148.1°. To inspect the dependence of the exchange coupling interaction on the Fe−O−Fe angle for $Cl_3FeOFeCl_3^{2-}$, $Cl_3Fe(OH)FeCl_3^{1-}$, and $Cl_3Fe(OH_2)FeCl_3$, the exchange coupling constants J with the change of the Fe−O−Fe angle are calculated by using DFT-BS method. Our calculated results reveal that the Fe−O−Fe angle does not have significant influence on the magnetic exchange interaction. Figure 2 is a plot of the calculated $-J$ versus the Fe−O−Fe angle for $Cl_3FeOFeCl_3^{2-}$, $Cl_3Fe(OH)FeCl_3^{1-}$, and $Cl_3Fe(OH_2)$-$FeCl_3$. From Figure 2, it is shown that the exchange coupling constants $-J$ for $Cl_3FeOFeCl_3^{2-}$ is only changed by 7 cm^{-1} with the Fe−O−Fe angle changed from 133° to 153°. The variant range of this angle in our calculations is chosen to correspond to the sharp change range in the plot of total energy versus the Fe−O−Fe angle reported by Rappe et al.[7c] For $Cl_3Fe(OH)FeCl_3^{1-}$ and $Cl_3Fe(OH_2)FeCl_3$, the variation of $-J$ is also nearly constant within 133° to 153°, about 11 cm^{-1} for the former and about 9 cm^{-1} for the latter. It is suggested that $-J$ is insensitive to the Fe−O−Fe angle for the μ-oxo, μ-hydroxo, and μ-aqua bridged iron(III) dimers, contrasted to the hydroxo-bridged copper(II) dimers, where a linear variation of J with Cu−O−Cu angle has been obtained experimentally and theoretically.[4e] In the case of the hydroxo-bridged copper-(II) dimers for Cu−O−Cu > 97.5°, the ground state is a singlet; however, when Cu−O−Cu < 97.5°, the ground state becomes a triplet. In a recent paper, Castell and Caballol[5a] reported the magnetic-structural dependence for the hydroxo doubly bridged Cr(III) dimer. Their ab initio calculations showed that the

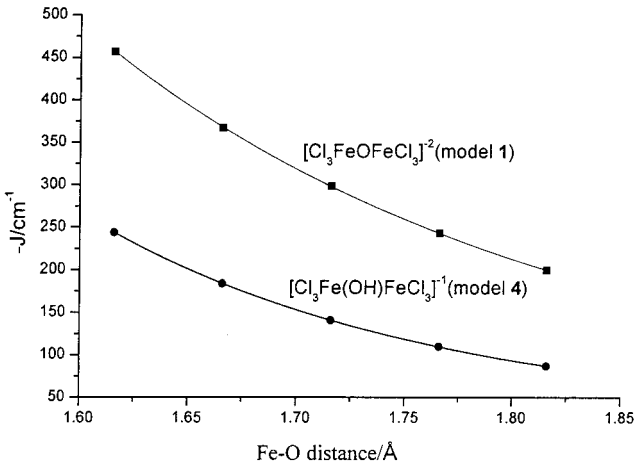

Figure 3. Dependence of the calculated magnetic coupling constants J of $[Cl_3FeOFeCl_3]^{2-}$ and $Cl_3Fe(OH)FeCl_3^{1-}$ on Fe−O distance.

dependence of the magnetic coupling constant J on the Cr−O−Cr angle is near parabolic with a maximum of −5 cm^{-1} corresponding to an angle of about 105° when the bridge angle ranges between 90° and 120°. It is evident that there is diversity in dependence of exchange coupling interaction on the bridge angle for oxo- and hydroxo-bridged transition-metal dimers. Our results on the angular dependence are in agreement with that reported by Rappe.[7c]

Figure 3 is a plot of the calculated $-J$ versus the Fe−O distance for $Cl_3FeOFeCl_3^{2-}$ and $Cl_3Fe(OH)FeCl_3^{1-}$. Their $-J$ values (in cm^{-1}) are calculated to be proportional to the following exponential functions of the Fe−O distance respectively,

$$-J = 3.581 \times 10^5 \exp(-4.129r) \quad (4)$$

and

$$-J = 1.219 \times 10^6 \exp(-5.274r) \quad (5)$$

Equation 4 is for $Cl_3FeOFeCl_3^{2-}$ and eq 5 is for $Cl_3Fe(OH)Fe$-Cl_3^{1-}, where r is the Fe−O distance in Å. The correlation coefficients are 0.9997 and 0.9987 for $Cl_3FeOFeCl_3^{2-}$ and $Cl_3Fe(OH)FeCl_3^{1-}$, respectively, ranging from 1.616 to 1.816 Å. Varying the Fe−O distance by 0.2 Å, from 1.616 to 1.816 Å, results in a variation of 257 cm^{-1} for J of $Cl_3FeOFeCl_3^{2-}$ and 157 cm^{-1} for J of $Cl_3Fe(OH)FeCl_3^{1-}$. The $-J$ value increases sharply as the Fe−O distance is shortened. The similar sensitive dependence of exchange coupling interaction on the Fe−O distance has also been recently reported.[7c] Rappe et al. found the J value to vary as the fourth power of the orbital overlap between the metal and ligand. Weihe and Gudel[7a] obtained the following angle and distance dependence of J (in cm^{-1}) in Hamiltonian $\hat{H} = J\hat{S}_1 \cdot \hat{S}_2$:

$$J = 1.337 \times 10^8 (3.536 + 2.488 \cos\phi + \cos^2\phi) \exp(-7.909r) \quad (6)$$

where r is the metal-bridge distance (in Å). It is obvious that this conclusion indicates a sensitive dependence of exchange coupling interaction on the Fe−O distance.

E. Molecular Orbital Analysis. *Frontier Orbital Component.* Figures 4 and 5 are diagrams of molecular orbital energy levels of the broken symmetry state for $Cl_3FeOFeCl_3^{2-}$ and $Cl_3Fe(OH)$-$FeCl_3^{1-}$. According to the classification proposed by Noodleman,[8d] these level diagrams belong to the mixed level scheme. There exists a thorough mixing of metal−ligand character in these

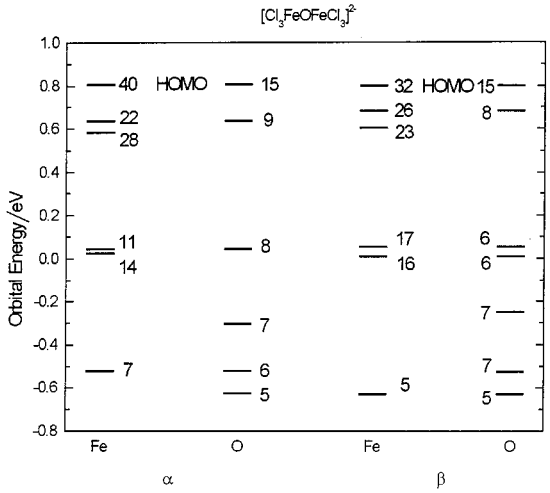

Figure 4. Orbital energy level and orbital component of the broken symmetry state for $[Cl_3FeOFeCl_3]^{2-}$. Digital in an energy level indicates the orbital component of the level. The components less than 5% and component of the terminal ligand Cl are omitted.

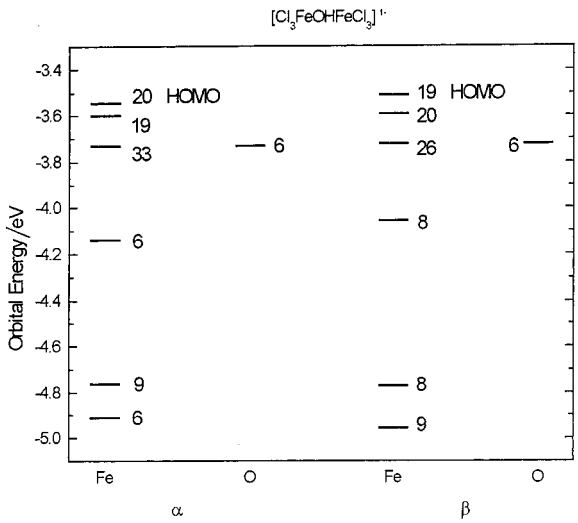

Figure 5. Orbital energy level and orbital component of the broken symmetry state for $[Cl_3Fe(OH)FeCl_3]^{1-}$. Digital in an energy level indicates the orbital component of the level. The components less than 5% and component of the terminal ligand Cl are omitted.

occupied frontier molecular orbitals. In comparison of Figure 4 and Figure 5, the protonation of the μ-oxo ligand in $Cl_3FeOFeCl_3^{2-}$ leads to decrease the level of bonding OH orbital, compared with the lone-pair electron orbital of the μ-oxo ligand and leads to induce a sharp decrease of the orbital components of the bridge O atom in the occupied frontier orbitals for $Cl_3Fe(OH)FeCl_3^{1-}$. As shown above, in these iron(III) dimers, the magnetic exchange interaction is a superexchange interaction through the bridging ligand. Thus, the decrease of the component of the bridge O atom in the occupied frontier molecular orbitals must lead to weaken the superexchange interaction between the two iron(III) centers. In the case of model **5**, again another proton attached decreases the level of the second lone-pair electron orbital of the bridge O atom through forming the second O−H bond, and the further decreases of the component of the bridge O atom in the occupied frontier molecular orbitals further weakens the magnetic exchange interaction.

Mulliken Overlap Spin Population Analysis. As shown above, in the occupied frontier molecular orbitals there exists a thorough mixture of atomic orbital characters from the metal and bridge ligand. This mixture leads a magnetic exchange interaction between the two iron(III) centers through the bridge. In the molecular orbital interaction theory, the interaction degree between two atoms can be described in term of the Mulliken overlap population M_{AB}

$$M_{AB} = \sum_{\mu\nu} P_{\mu\nu} S_{\mu\nu} \tag{7}$$

where $P_{\mu\nu}$ and $S_{\mu\nu}$ indicate density matrix and overlap matrix, respectively. In unrestricted DFT calculation, Mulliken overlap spin population M^s_{AB} is as follows:

$$M^s_{AB} = \sum_{\mu\nu} P^s_{\mu\nu} S_{\mu\nu} \tag{8}$$

$$P^s_{\mu\nu} = P^\alpha_{\mu\nu} - P^\beta_{\mu\nu} \tag{9}$$

where α and β indicate the electronic spin state. Table 1 lists the distance of Fe−O, the calculated $-J$ value, and the Mulliken overlap spin population of Fe−O(oxo), M^s_{Fe-O}, for the models **1**, **4**, **5**, **6**, **6′**, **7**, and **7′** in their high spin state. It is found that there exists, indeed, a very close relationship between the magnetic exchange coupling of the two iron(III) centers and the Mulliken overlap spin population of Fe−O. In the case of $Cl_3FeOFeCl_3^{2-}$ with different Fe−O distances, the calculated $-J$ value is linearly proportional to M^s_{Fe-O} ($\times 10^{-3}$).

$$M^s_{Fe-O} = 114.06 - 0.2552J \tag{10}$$

J is the exchange coupling constant in cm^{-1}. The regression coefficient is 0.9995, ranging from 200 to 457 cm^{-1} for the $-J$ values, corresponding to the range of Fe−O distance from 1.816 Å to 1.616 Å. Figure 6 shows the linear correlation between the calculated $-J$ and M^s_{Fe-O} ($\times 10^3$) for $Cl_3FeOFeCl_3^{2-}$. Comparison of the calculated M^s_{Fe-O} value shows the smaller M^s_{Fe-O} values of models **4** (0.114) and **5** (0.067) compared with model **1** (0.176), the smaller M^s_{Fe-O} value of model **5**

TABLE 1: Fe−O Distance, the Calculated $-J$ and Mulliken Overlap Spin Population M^s_{Fe-O}

	Fe−O (Å)	$-J$ (cm^{-1})	M^s_{Fe-O}
$Cl_3FeOFeCl_3$ (**1**)	1.616	457	0.230
	1.666	367	0.209
	1.716	298	0.191
	1.766	243	0.176
	1.816	200	0.164
$Cl_3Fe(OH)FeCl_3$ (**4**)	1.765	110	0.114
$Cl_3Fe(OH_2)FeCl_3$ (**5**)	1.765	62	0.067
$(NH_3)_3FeO(CH_3COO)_2Fe(NH_3)_3$ (**6**)	1.784	329	0.182
$(NH_3)_3Fe(OH)(CH_3COO)_2Fe(NH_3)_3$ (**6′**)	1.784	189	0.097
$(NH_3)_3Fe(OH)(CH_3COO)_2Fe(NH_3)_3$ (**7**)	1.956	75	0.093
$(NH_3)_3FeO(CH_3COO)_2Fe(NH_3)_3$ (**7′**)	1.956	198	0.162

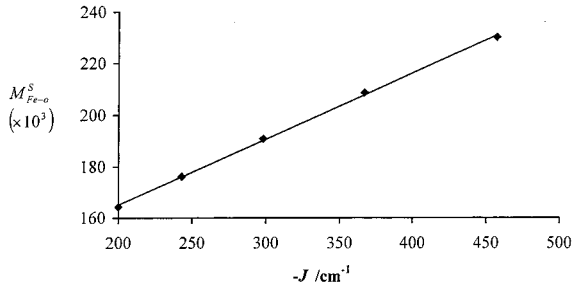

Figure 6. Plot of Mulliken overlap spin population M^S_{Fe-O} vs the calculated $-J$ value.

TABLE 2: The Partial Optimized Geometry, Full Optimized Geometry, and Calculated *J* Value for Models 1, 1′; 4, 4′; 5, 5′

	model **1**	model **1′**	model **4**	model **4′**	model **5**	model **5′**
Fe−O (Å)	1.766	1.834	1.766	1.988	1.766	2.315
Fe−Cl (Å)	2.217−2.238	2.267−2.293	2.217−2.238	2.195−2.222	2.217−2.238	2.150−2.181
O−H (Å)			0.98	0.98	0.999	0.986
Fe−O−Fe (°)	148	150	148	143	148	144
H−O−H (°)					114.6	104.3
J (cm^{-1})	−243	−177	−110	−49	−62	−11

(0.067) compared with model **4** (0.114), the smaller M^s_{Fe-O} value of model **6′** (0.097) compared to model **6** (0.182), and the smaller M^s_{Fe-O} value of model **7** (0.093) compared to model **7′** (0.162). These calculated M^s_{Fe-O} values indeed are correlated well to the calculated J values. It appears that the qualitative discussion of the dependence of the magnetic coupling J value on chemical and structural variations can be based on the Mulliken overlap spin population analysis. The discussion above is based on the Mulliken overlap spin population analysis of the high spin state for the model compounds studied. The case is true for the broken symmetry state. Recently, Ruiz et al. also reported an excellent correlation between the overlap spin population and the calculated J values for carboxylato-bridged dinuclear copper(II) compounds.[15]

F. Geometry Optimization of the Model and Magnetic Exchange Interaction. For models **4** and **5** studied above, the partial geometry optimization is performed only for positions of hydrogen atoms in hydroxo- and aqua-bridge ligands. Geometrical parameters of model **1** are directly taken from structural determination experimentally. To inspect the effect of geometry optimization on the magneto−structural correlation, full geometry optimization for models **1**, **4**, and **5** is performed with models **1**, **4**, and **5** to be taken as the initial geometry, leading the new models **1′**, **4′**, and **5′**, respectively.

Table 2 lists the selected optimized bond lengths and bond angles as well as the calculated exchange coupling constants J by using the DFT-BS method. All the Fe−Cl distances optimized are not equal to each other because of the initial structure of model **1** without an ideal molecular symmetry, which is taken from the practical X-ray crystallography analysis. Table 2 reveals that after the full geometry optimization, the Fe−O in models **1′**, **4′**, and **5′** are all lengthened, from 1.766 Å in model **1** to 1.834, 1.998, and 2.315 Å, respectively, for models **1′**, **4′**, and **5′**. The Fe−Cl distance exhibits different behavior. The Fe−Cl distances in model **1′** are lengthened from 2.217−2.238 Å to 2.267−2.293 Å. However, for models **4′** and **5′**, these Fe−Cl distances are shortened to 2.195−2.222 Å and 2.150−2.181 Å, respectively. On the other hand, the O−H distances in models **4′** and **5′** have unremarked variance in the geometry optimization. As far as variation of bond angles is concerned, the Fe−O−Fe angle in model **1′** is 2° larger than in model **1**, but in the case of models **4′** and **5′**, the Fe−O−Fe angles are 143° and 144°, respectively, less than 148° in model **1**. It appears that the full geometry optimization for models **4** and **5** does not simply lengthen bond distances and increase bond angles. Also, Table 2 shows that models **1′**, **4′**, and **5′** optimized have a weaker anti-ferromagnetic interaction comparing with models **1**, **4**, and **5**. The decrease of the corresponding coupling constant J in absolute value should be attributed to the longer Fe−O distance in models **1′**, **4′**, and **5′** optimized.

To examine the validity of the magneto−structural correlation obtained from models **1**, **4**, and **5** studied above, the exchange coupling constants J with change of the Fe−O−Fe angle and the Fe−O distance are again calculated by using DFT-BS method for models **1′**, **4′**, and **5′**. Figure 7 is a plot of the calculated $-J$ value versus the Fe−O−Fe angle for $Cl_3FeOFeCl_3^{2-}$, $Cl_3Fe(OH)FeCl_3^{1-}$, and $Cl_3Fe(OH_2)FeCl_3$ optimized. Figure 7 reveals obviously that after the full geometry optimization, the $-J$ value is also insensitive to the Fe−O−Fe angle for the -oxo, -hydroxo and -aqua bridged iron(III) dimers, and the same dependence of the J value on the Fe−O−Fe angle is obtained as in the case of models **1**, **4**, and **5**. The dependence of the J value on the Fe−O distance for models **4′**, and **5′** is also established to be proportional to an exponential function of the Fe−O distance as follows, respectively,

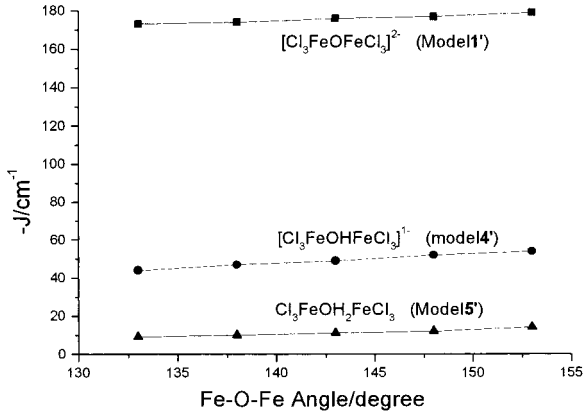

Figure 7. Dependence of the calculated magnetic coupling constants J in models **1′**, **4′**, and **5′** optimized on Fe−O−Fe angle.

$$-J = 9.15 \times 10^5 \exp(-4.0r) \quad (11)$$

and

$$-J = 1.86 \times 10^5 \exp(-3.6r) \quad (12)$$

where r is also the Fe−O distance in Å, and J is in cm^{-1}. Thus, the validity of the dependence of the exchange coupling constant J on the bridge angle and bridge distance, obtained from the models with partial geometry optimization, is further confirmed though equations 11 and 12 have a different power B and factor A in eq 1 from equations 4 and 5. It is shown that the model method with the partial geometry optimization is a useful approach in study on qualitative magneto−structural correlation, especially to larger molecules.

Conclusions

The calculated results show that DFT-BS method indeed provides a useful and practicable approach for the dependence of magnetic exchange interaction between the two bridged metal centers on variation of the chemical nature and structure of the bridge. In the present paper, the calculated magnetic coupling constants agree with experimental observation for the bridged-transition-metal dimers with five unpaired electrons on each metal center. These oxo-bridged iron(III) dimer systems studied obviously increase electronic complexity compared to the bridged Cu(II) dimer and the bridged Cr(III) dimer. The former has only one unpaired electron on each Cu(III) center, and the latter has three unpaired electrons on each Cr(III) center.

The magneto−structural correlation for the bridged-transition-metal dimers is diversity. For the μ-oxo bridged iron(III) dimer, the dependence of the exchange coupling constants on the Fe−O(oxo)-Fe angle is insensitive; on the other hand, the dependence of exchange coupling interaction on the Fe−O distance can be expressed as an exponential function of the Fe−O distance. Furthermore, the protonation of the μ-oxo ligand, leading to form a μ-hydroxo ligand, causes sharp decrease of the exchange coupling interaction. However, in the case of the μ-hydroxo bridged Cu(II) dimers and Cr(III) dimers, the situations are quite different from the Fe(III) dimers. For the μ-hydroxo bridged Cu(II) dimers, there is a linear variation of J with a Cu−O−Cu angle, and for the μ-hydroxo doubly bridged Cr(III) dimers, the dependence of the magnetic coupling constant J on the Cr−O−Cr angle is near parabolic.

Molecular orbital interaction theory is invoked to explain the magneto−structural correlation of the μ-oxo bridged iron(III) dimers. It is shown in our calculations that the Mulliken overlap spin populations are related to the variation of the exchange coupling constants J in the protonation of the μ-oxo bridge ligand and to the variations of the bridge angle and bridge distance. For the systems mentioned, such as μ-hydroxo bridged Cu(II) dimers, μ-hydroxo doubly bridged Cr(III) dimers, and μ-oxo bridged Fe(III) dimers, the molecular orbital interaction is a dominant factor in their anti-ferromagnetic coupling. However, because the spin coupling between the two metal magnetic centers is a very weak interaction, it is difficult to do that all complicated situations of the magnetic exchange interaction in molecules are attributed to the simpler molecular orbital interaction. Finally, the validity in qualitative magneto−structural correlation for the models used is further confirmed by full geometry optimization.

Acknowledgment. The authors thank Dr. Louis Noodleman (The Scripps research Institute, USA) and Dr. Jian Li for their informative discussion on the broken symmetry approach. The authors Chen, Zhang, and Yan are grateful to the National Science Foundation of China (29831010, 20023005) and the State Key Project of Fundamental Research of China (G199806-1306).

References and Notes

(1) Gatteschi, D.; Kahn, O.; Miller, J. S.; Palacio, F. *Magnetic Molecular Materials*; Kluwer Academic: Dordrecht, The Netherlands, 1991.

(2) Kahn, O.; Pei, Y.; Journaux, Y. In *Inorganic Materials*; Bruce, Q. W., O'Hare, D., Eds.; John Wiley & Sons: Chicheter, U.K., 1992.

(3) Kahn, O. *Molecular Magnetism*; VCH Publisher: New York, 1993.

(4) (a) Blanchet-Boiteux, C.; Mouesca, J. *J. Am. Chem. Soc.* **2000**, *122*, 861. (b) Adamo, C.; Barone, V.; Bencini, A.; Totti, F.; Ciofini, I. *Inorg. Chem.* **1999**, *38*, 1996. (c) Aebersold, M. A.; Gillon, B.; Plantevin, O.; Pardi, L.; Kahn, O.; Bergerat, P.; von Seggern, I.; Tuczek, F.; Ohrstrom, L.; Grand, A.; Lelievre-Brena, E. *J. Am. Chem. Soc.* **1998**, *120*, 5238. (d) Ruiz, E.; Cano, J.; Alvarez, S.; Alemany, P. *J. Am. Chem. Soc.* **1998**, *120*, 11122. (e) Ruiz, E.; Alemany, P.; Alvarez, S.; Cano, J. *J. Am. Chem. Soc.* **1997**, *119*, 1297. (f) Ruiz, E.; Alemany, P.; Alvarez, S.; Cano, J. *Inorg. Chem.* **1997**, *36*, 3683. (g) Cano, J.; Alemany, P.; Alvarez, S.; Ruiz, E.; Verdaguer, M. *Chem. Eur. J.* **1998**, *4*, 476. (h) Erasmus, C.; Haase, W. *Spectrochim. Acta* **1994**, *50A*, 2189. (i) Daudey, J. P.; de Loth, P.; Malrieu, J. P. In *Magneto-Structural Correlations in Exchange Coupled Systems*; Willett, R. D., Gatteschi, D., Kahn, O., Eds.; Kluwer Academic Publishers: Dordrecht, The Netherlands, **1985**; Vol. 140.

(5) (a) Castell, O.; Caballol, R. *Inorg. Chem.* **1999**, *38*, 668. (b) Hodgson, D. J. In *Magneto Structural Correlations in exchange Coupled Systems*; Willett, R. D., Gatteschi, D., Kahn, O., Eds.; NATO Advanced Studies Series C.; Reidel: Dordrecht, The Netherlands, 1985; Vol. 140, p 497. (c) Scaringe, R. P.; Hodgson, D. J.; Hatfield, W. E. *Transition Met. Chem.* **1981**, *6*, 340. (d) Glerup, J.; Hodgson, D. J.; Pedersen, E. *Acta Chem. Scand., Ser. A* **1983**, *37A*, 161.

(6) (a) Kurtz, D. M., Jr. *Chem. Rev.* **1990**, *90*, 585. (b) Turwski, P. N.; Armstrong, W. H.; Liu, S.; Brown, S. N.; Lippard, S. J. *Inorg. Chem.* **1994**, *33*, 636. (c) Haselhorst, G.; Wieghardt, K.; Keller, S.; Schrader, B. *Inorg. Chem.* **1993**, *32*, 520. (d) Chaudhuri, P.; Wieghardt, K.; Nuber, B.; Weiss, J. *Angew Chem., Int. Ed. Engl.* **1985**, *24*, 778. (e) Amstrong, W. H.; Lippard, S. J. *J. Am. Chem. Soc.* **1984**, *106*, 4632. (f) Weiss, H.; Strahle J. *Z. Naturforsch., Teil B*, **1984**, *39*, 1453. (g) Armstrong, W. H.; Spool, A.; Papaefthymiou, G. C.; Frankel, R. B.; Lippard, S. J. *J. Am. Chem. Soc.* **1984**, *106*, 3653.

(7) (a) Weihe, H.; Gudel, H. U. *J. Am. Chem. Soc.* **1997**, *119*, 6539. (b) Hazell, A.; Jensen, K. B.; McKenzie, C. J.; Toftlund, H. *Inorg. Chem.* **1994**, *33*, 3127. (c) Hart, J. R.; Rappe, A. K.; Gorun, S. M.; Upton, T. H. *Inorg. Chem.* **1992**, *31*, 5254. (d) Gorun, S. M.; Lippard, S. J. *Inorg. Chem.* **1991**, *30*, 1625. (e) Mukherjee, R. N.; Stack, T. D. P.; Holm, R. H. *J. Am. Chem. Soc.* **1988**, *110*, 1850. (f) Mabbs, F. E.; McLachlan, V. N.; McFadden, D.; McPhail, A. T. *J. Chem. Soc., Dalton Trans.* **1973**, 2016. (g) Gerloch, M.; Towl, A. D. C. *J. Chem. Soc. A* **1969**, 2850. (h) Hay, P. J.; Thibeault, J. C.; Hoffmann, R. *J. Am. Chem. Soc.* **1975**, *97*, 4884. (i) Norman, R. E.; Yan, S.; Que, L.; Backes, G.; Ling, L.; Sanders-Loehr, J.; Zhang, J. H.; O'Connor, C. J. *J. Am. Chem. Soc.* **1990**, *112*, 1554.

(8) (a) Noodleman, L. *J. Chem. Phys.* **1981**, *74*, 5737. (b) Noodleman, L.; Baerends, E. J. *J. Am. Chem. Soc.* **1984**, *106*, 2316. (c) Noodleman, L.; Case, D. A. *Adv. Inorg. Chem.* **1992**, *38*, 423. (d) Li, J.; Noodleman, L.; Case, D. A. In *Inorganic Electronic Structure and Spectroscopy*; Solomon, E. I., Lever, A. B. P., Eds.; Wiley: New York, **1999**; Vol. 1, pp 661−724.

(9) Yan, B.; Chen, Z.; Wang, S. *J. Chin. Chem. Soc.* **2000**, 47, 1211.

(10) *Amsterdam Density Functional (ADF)*, revision 2.3; Scientific Computing and Modelling, Theoretical Chemistry, Virje Universiteit: Amsterdam, The Netherlands, 1997.

(11) Vosko, S. H.; Wilk, L.; Nusair, M. *Can. J. Phys.* **1980**, *58*, 1200.

(12) Becke, A. D. *Phys. Rev. A* **1988**, *38*, 3098.

(13) Perdew, J. P. *Phys. Rev. B* **1986**, *33*, 8822.

(14) (a) Boerrigter, P. M.; Velde, G. T.; Baerends, E. J. *Int. J. Quantum Chem.* **1988**, *33*, 87. (b) Velde, G. T.; Baelends, E. J. *J. Comput. Phys.* **1992**, *99*, 84.

(15) Rodriguez-Fortea, A.; Alemany, P.; Alvarez, S.; Ruiz, E. *Chem. Eur. J.* **2001**, *7*, 627.